European Journal of Wood and Wood Products (2025) 83:159
https://doi.org/10.1007/s00107-025-02314-z

ORIGINAL ARTICLE

Observing accelerated chemical colour change in aspen and birch wood using hyperspectral imaging and spectrophotometry

Joona Lampela[1] · Markku Keinänen[2,3] · Antti Haapala[1] · Olusegun Akinyemi[1] · Veikko Möttönen[4]

Received: 30 November 2024 / Accepted: 1 August 2025
© The Author(s) 2025

Abstract
Natural weathering gradually turns wood light grey over years, driven by exposure to sunlight, precipitation, and biological agents. Nontoxic chemicals have been used to accelerate artificial weathering-induced colour changes in wood. This study aimed to evaluate the effectiveness and underlying mechanisms of various surface treatment chemicals and a commercial silicon-based product in accelerating UV-induced colour changes in birch and aspen under artificial weathering conditions. Weathering was conducted by using an artificial weathering testing instrument with or without spraying the samples with water. Colour changes were measured with a portable spectrophotometer. Hyperspectral imaging data were included to visualise spatial variations of colour in wood samples. The use of water was a significant factor in determining the colour change in wood. Mostly photodegraded lignin constituents leached out of the wood with water spraying but remained if it was not used. The treatment chemicals caused distinct colour changes: Iron (II) sulphate caused dark grey staining, citric acid a unique red colour, sodium hydroxide darkening and brown hue, and hydrogen peroxide the most uniform colour. Commercial silicon-based product caused either little or no noticeable colour change over control samples. The greatest potential for colour change occurred during the first hours of artificial weathering. Spatial data of hyperspectral images allowed for more accurate estimation of variability over spectrophotometer data, and use of hyperspectral imaging in further research is therefore suggested.

1 Introduction

Uncoated wooden structures exposed to long-term weathering develop a characteristic grey patina, often admired for its natural and rustic appearance. Grey weathered wood is pleasing to look at, and it is a natural building material, distinctly different from decayed or rotten wood. However, wood discolouring may take years to bring about the desired rustic finish under natural conditions. A common interest of architects and customers who are willing to use weathered wood in indoor or outdoor applications is to achieve the grey surface sooner rather than later.

Factors that contribute to weathering are solar radiation (ultraviolet and visible light), water, oxygen, temperature, air pollution, particulate matter, and microorganisms (Hon and Shiraishi 2001a, b; Rowell 2013). In addition to the colour change, the wood surface becomes rough and cracked. The main factor that drives the weathering of wood is solar radiation (Rowell 2013). Light-induced photochemical changes to the material's properties are referred to as photodegradation (Hon and Shiraishi 2001a, b). Lignin has a light absorption peak at 280 nm which is in the UVB spectrum and its tail extends over to the visible light region (Hon and Shiraishi 2001a, b). However, radiation above 295 nm is responsible for the photochemical reactions in wood since shorter wavelengths are absorbed by the Earth's ozone layer (Rowell 2005). Kataoka et al. (2007) concluded that violet light of visible light spectrum causes photodegradation whereas blue light causes bleaching but no degradation. Photochemical changes appear in all chemical constituents

✉ Veikko Möttönen
veikko.mottonen@luke.fi

1 Department of Chemistry and Sustainable Technology, University of Eastern Finland, P.O. Box 111, Joensuu 80101, Finland

2 Department of Environmental and Biological Sciences, University of Eastern Finland, P.O. Box 111, Joensuu 80101, Finland

3 Center for Photonics Sciences, University of Eastern Finland, P.O. Box 111, Joensuu 80101, Finland

4 Production systems, Natural Resources Institute Finland, Yliopistokatu 6B, Joensuu 80100, Finland

Published online: 22 August 2025

of wood. UV light can induce the formation of free radicals in wood constituents. Free radicals can cause discolouring reactions, because with the presence of oxygen, free radicals are short-lived and form hydrogen peroxides (Hon and Shiraishi 2001a, b; Rowell 2013). Quantum energies of UV light can cleave chemical bonds, such as C-C, C-O, and C-H bonds in wood constituents. Hon and Glasser (1979) classified these potential chromophoric or colour bearing groups, and they included phenolic hydroxyl groups, double bonds, carbonyl groups, different quinones, biphenyls, and chromophore free radicals. Several of these chromophoric elements are present in lignin, and lignin is known to be a good UV absorber (Fengel and Wegener 1984). Since lignin can absorb more photon energies than holocellulose, degradation primarily appears in lignin (Hon and Shiraishi 2001a, b). In a later study, Mitsui (2004) used various filters to study the effect of wavelength on heat-induced colour change. He noted differences for colour change with and without heat treatment and attributed this to different chemical reactions for UV irradiation at ambient temperature and UV at elevated temperature. The degree of colour change increased by decreasing wavelength. Some colour change was observed at 400–500 nm and it was attributed to colour change of extractives.

The presence of water further changes the chemical properties of photodegraded wood. Degraded lignin products such as quinones and hemicellulose sugars are leached from the wood by water. Due to leaching, initially yellowed or darkened wood becomes grey. Photodegraded and leached wood surface primarily constitutes cellulose. Further lightening of remaining cellulose is exerted by photo-oxidation caused by UV light and ambient oxygen molecules. However, without any precipitation, photodegradation products accumulate in the wood and cause wood to become darker in colour (Rowell 2013).

Spectrophotometers are widely used for colour measurements, and they measure material reflectance or transmission across the UV, visible, and near-infrared spectrum (Konica Minolta 2007). However, spectrophotometers are based on point measurements, and with spatially heterogeneous materials, the results depend on the location of the relatively small measurement area. Hyperspectral imaging (HSI) combines spectroscopy with imaging, providing spatial information on the variation of spectral reflectance, thus making it suitable for spectroscopic studies of heterogeneous materials such as wood. Several studies have investigated the weathering of wood with spectrophotometers (Jankowska and Kwiatkowski 2022; Jankowska et al. 2017; Miklecic and Jirous-Rajkovic 2011; Park et al. 2018; Dagher et al. 2022), chroma meters (Özçifçi and Özbay 2010), scanners (Hundhausen et al. 2020; Lesar and Humar 2022; Lesar et al. 2024), and hyperspectral cameras (Herrera et al. 2018; Jordan et al. 2022; Sandak et al. 2017). However, there are few studies on how to accelerate the weathering-induced colour change in wood.

The aims of this study were to investigate artificial weathering-induced colour changes in birch (*Betula pendula* Roth) and aspen (*Populus tremula* L.) wood using nontoxic chemicals and to evaluate the underlying reasons behind induced colour changes with special interest towards grey colour. In addition, the aim of this study was to compare the capabilities of spectrophotometry and hyperspectral imaging (HSI) in monitoring and quantifying colour change and spatial heterogeneity across chemically treated wood samples, thereby evaluating the added value of HSI in wood surface analysis.

2 Materials and methods

2.1 Sample preparation

The natural and commercially utilized Nordic hardwood species used in this study were Eurasian aspen (*Populus tremula* L.) and silver birch (*Betula pendula* Roth). European aspen and silver birch were selected because they are the most common hardwood species in Finland, and there could be commercial potential for improving their added value through modification treatment. However, due to their susceptibility to decay, applications would be in outdoor conditions where they are not in contact with water or soil. Mature wood blocks were kept under temperature and humidity conditions indoors for two weeks prior to sample preparation. Then, they were sawn and planed to dimensions of 50 mm × 75 mm × 8 mm. Specimens that contained any visible defects, such as knots and pitch pockets, were discarded. A total of 3 batches were prepared for artificial weathering and their replicate amounts can be seen in Table 1.

Five surface treatment chemicals were applied to the samples: citric acid ($C_6H_8O_7$, Cit), sodium hydroxide (NaOH, NaOH), iron (II) sulphate ($FeSO_4$, Fe), hydrogen peroxide (H_2O_2, H2O2), and commercial OrganoWood® Wood Protection 1 (Osm). According to the OrganoWood® safety data sheet, the product is alkaline (pH 10.0—11.4) water-based mixture of inorganic polymer and organic acid. The treatment is claimed to cause discolouration on wood, with light, silver-grey finish. The product also claims improved protection by encapsulating wood fibres with silicon molecules. Additionally, a control group (Con) without surface treatment was used. Surface treatment agents were mixed with distilled water, except commercial Osm, which was used as received. Cit and Fe concentrations were 50% w/v. NaOH solution containing 1% sodium hydroxide and

Table 1 Number of wood samples by species and treatment type

Wood species	Treatment	Batch	
		Dry	Wet
Aspen	Con	3	3
	H2O2	3	3
	Osm	3	3
	Cit	3	3
	NaOH	3	3
	Fe	3	3
Birch	Con	2	3
	H2O2	4	3
	Osm	4	3
	Cit	3	3
	NaOH	4	3
	Fe	4	3
Total		39	36

4% hydrogen peroxide w/v was used in batch (1) Due to unsatisfactory discolouration results, the formulation was adjusted to 10% sodium hydroxide without hydrogen peroxide in batch (2) For H_2O_2, the initial concentration was set to 10% w/v of hydrogen peroxide, but in the following batch 2, the concentration was set to 50%. High concentrations of treatment chemicals were used because the aim of this study was to inflict distinct and strong colour changes. The surface treatment of the samples was conducted within an hour with paint brushes on one 75 mm × 50 mm side of a sample. The samples were painted twice and left untouched until the treatment chemicals had been absorbed. After an absorption time of 5–10 min, the samples were left to stand in a dark and dry environment for a minimum of 24 h on their 75 mm × 8 mm side to be dried.

2.2 Artificial weathering

Artificial weathering was conducted according to ISO 16474-2 (2013) with an Atlas Xenotest® 440 weathering instrument (Ametek Inc., Baton Rouge, LA, USA) equipped with two 2200 W air cooled xenon lamps. The xenon lamps radiate UV light, visible light, and infrared radiation mimicking natural daylight. The samples were attached to stainless steel racks, which were then mounted on a spherical carousel surrounding the xenon lamps. Altered parameters in the 2 batches used in this study included water spraying, relative humidity, and time of the complete weathering cycle which are described in Table 2. Artificial weathering periods for the two batches, lasted for 96 h and 522 h, respectively and their UV-radiation energy exposures were 20.74 MJ/m^2 and 112.75 MJ/m^2, respectively with power of 60 W/m^2. Weathering periods contained sub cycles 1 and 2. For batch 1, sub cycle 1 lasted for 102 min and sub cycle 2 for 18 min, and for batch 2 correspondingly 462 min and 18 min. To aid distinguish weathering conditions, batch 1 is referred to as dry batch, because no rain was used during its weathering. Relative humidity for dry batch was set to 95%. For batch 2 sub cycle 1 relative humidity was set to 50% min and during sub cycle 2 rain was used. Batch 2 is referred to as wet batch. The amount of sprayed water was 1.2 l/min for each batch.

2.3 Colour measurements and hyperspectral imaging

Colour measurement of the wood samples was conducted in the UVA and visible light wavelength range of 360–740 nm with a Konica Minolta 2600d portable spectrophotometer (Konica Minolta Inc., Tokyo, Japan). Spectral data were converted to CIEL*a*b* colour coordinates. Measurements were conducted before, during, and after the artificial weathering process. Singular measurement locations of 8 mm diameter were selected at the centre of the samples, avoiding cracks that might have originated during artificial weathering.

Hyperspectral and RGB (red, green, and blue) images were taken with a Specim IQ hyperspectral camera (Specim, Spectral Imaging Ltd). The camera collects 204 spectral bands with a spectral resolution of 7 nm (FWHM) and a spatial resolution of 512 × 512 pixels at 400–1000 nm (VNIR), with 31° field of view. The device has a 5 Mpix viewfinder camera, which is rescaled to 1280 × 960 pix. The Specim IQ camera was mounted on a stand positioned to point directly downward. A black matte-surfaced pedestal was set right under the camera, and the distance between the camera and the pedestal was 47.5 cm. Imaging objects were illuminated with six 35 W Osram Decostar 51 Alu tungsten halogen lamps directed at a 45° angle towards the pedestal from a distance of 40 cm. An adjustable bench power supply (EA PS2342-10B, Elektro-Automatik, Germany) supplied stabilized 12 V DC power for the light fixture. Before each image shoot, the lamps were stabilised for approximately 15 min, and a white reference image was taken. For quality control, the white reference was imaged also after each imaging session. Dark current references were automatically acquired by the camera. Flat field correction for reflectance calibration was conducted with the Fiji distribution of

Table 2 Description of weathering parameters used in the different weathering batches

Batch	Time (h)	Sub cycle 1 + 2 (min)	RH of sub cycle 1 (%)	RH of sub cycle 2 (%)	UV radiant exposure MJ/m^2	Description
Dry	96	102 + 18	95	95	20.74	No rain, RH 95
Wet	522	462 + 18	50	Rain	112.75	Long cycle, less frequent rain

ImageJ software (Schindelin et al. 2012), and image processing and analysis in Spectronon hyperspectral software (Resonon Inc., Bozeman, USA). The same settings were used for all measurement times.

3 Results and discussion

3.1 Visible light reflectance spectra of wood

Prior to artificial weathering, the reflectance of the samples in the UV range (360–400 nm) was low (5–15%, Fig. 1), indicating strong absorption by chromophoric compounds – primarily lignin – within the wood matrix (Hon and Shiraishi 2001a, b; Fengel and Wegener 1984). Lignin absorbs strongly radiation in the UV range and lignin-based anti-UV functional materials have been rigorously studied in recent years (Lv et al. 2023). The reflectance was greater in the visible light region (above 400 nm), gradually increasing with wavelength and reaching the maximum in the red region (720 nm). The shift of colours from green to red contributes to the characteristic brown colouration of wood. Compared to birch samples, the reflectance spectra of unweathered aspen showed a steeper slope and higher reflectance particularly in the wavelength range from green to yellow (550–600 nm), resulting in lighter appearance of aspen wood samples. The H2O2 treatment resulted in the highest reflectance before artificial weathering, followed by Con, Cit, Osm, Fe, and NaOH treatments (Fig. 1). With aspen, the differences in reflectance between treatments were largest at 460 nm but gradually decreased towards the infrared region. With birch, H2O2 and Con treated samples showed the highest reflectance. There was considerable heterogeneity in the samples, due to e.g., variation in earlywood and latewood, and variation in the drying result of the chemical treatment. Therefore, 8 mm point measurements may not accurately represent the reflectance spectrum of the sample.

After the artificial weathering process including water spraying, reflectance in the UV region increased for all sample treatments (Fig. 1), which indicates photodegradation and leaching of UV-absorbing components, such as lignin, as expected (Rowell 2013). The spectra of aspen H2O2, Con, Cit, and Osm samples resembled each other and showed a tendency for decrease in reflectance at about 500 to 600 nm. In birch samples, the H2O2 and Cit treatments showed the highest reflectance, followed by Osm and Con samples. With both species, NaOH and Fe treatments resulted in lowest reflectance across the whole range.

Artificial weathering without water does not lead to the leaching of photodegraded components, and thus, does not simulate natural outdoor conditions. Consequently, in the UV region, the reflectance of the samples either remained the same or decreased only slightly (Fig. 1), indicating that the photodegraded chromophoric lignin constituents were still present in the samples. In the visible light and infrared regions, the reflectance decreased particularly at wavelengths of 400 to 560 nm, but remained relatively high at longer wavelengths, causing the wood samples to become more yellowish, as has been reported for photodegradation of wood under indoor conditions (Hon and Shiraishi 2001a, b). The reflectance of Fe-treated samples did not show a similar trend, but rather resulted in an overall decrease in reflectance and greyish appearance (Fig. 1). With both wood species, Cit treatment resulted in a strong decrease at shorter wavelengths up to about 630 nm, giving the samples a reddish brown appearance.

3.2 Gradual colour change in CIELAB colour space

In dry batch, the largest decrease in lightness (L*) was observed for all treatment chemicals during the first day of weathering period (Fig. 2). The decrease in lightness continued from then until the end of the weathering (48 h), but at a significantly slower rate. The decrease in lightness was greatest with Cit, Fe, NaOH and Osm treatments. The change in lightness was similar in both wood species, with a slightly higher values for birch. In the industrial production of artificially weathered wood, achieving the desired weathered appearance rapidly is critical for economic viability.

Changes in redness (a*) and yellowness (b*) in the dry batch were also greatest during the first day (Fig. 3). Both colour values increased with all treatments except with aspen wood with Fe treatment. The wood species did not differ significantly from each other with respect to the different treatment chemicals. Generally, yellowness increased more than redness, except in the Cit treatment, where the increase in redness was strong in both wood species.

In the wet batch, lightness decreased the most on the first day, as in the dry batch (Fig. 2). However, the decrease in lightness stopped after 1—3 days and then remained at the same level or began to increase towards the end of the treatment. The highest changes in lightness were seen in Fe and NaOH samples, and especially when compared to Con. In birch, the lightness was higher at the end than at the beginning with Cit, Osm and H2O2 treatments, and in aspen with Osm treatment.

Regarding redness and yellowness, the wet batch differed from the dry batch, as the changes on the first day differed between the different treatment chemicals (Fig. 3). There were also more differences between the wood species than in the dry batch. Redness and yellowness increased during the first day only in the control samples and in the NaOH and Cit treatments. In birch, redness decreased until the end of the wet batch, being at a lower level than at the beginning

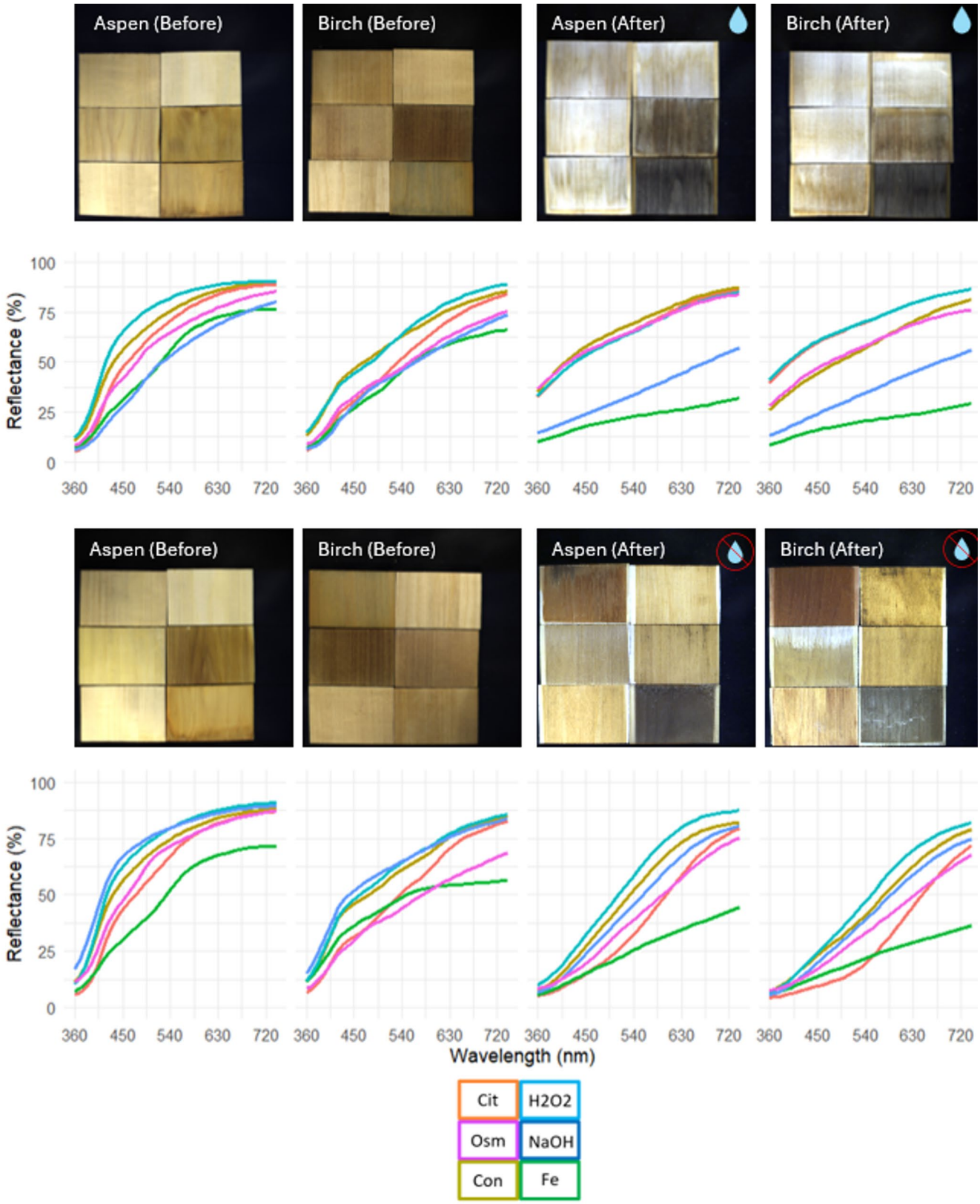

Fig. 1 RGB images of batch 1 (bottom) and 2 (top) samples before (leftmost) and after (rightmost) artificial weathering. The images were recorded with an RGB camera of HSI and mean spectral reflectance curves were measured with a spectrophotometer

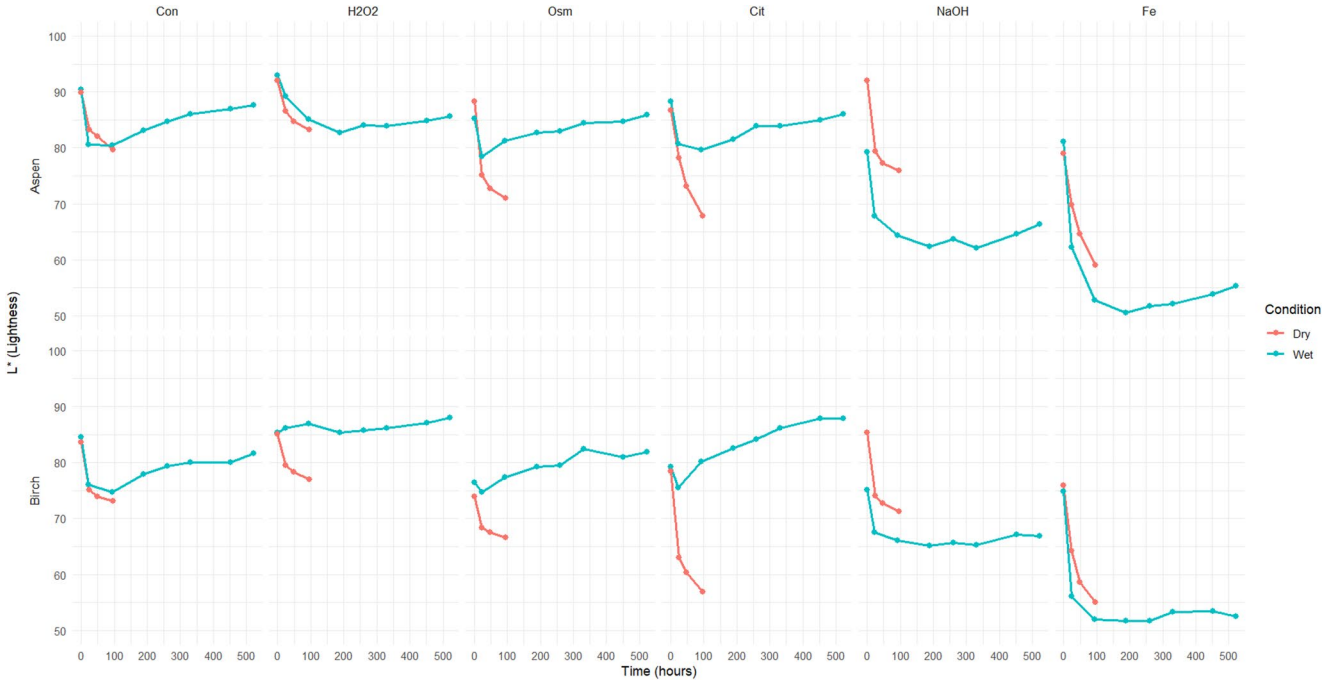

Fig. 2 Evolution of lightness (L*) by species, treatment and batch

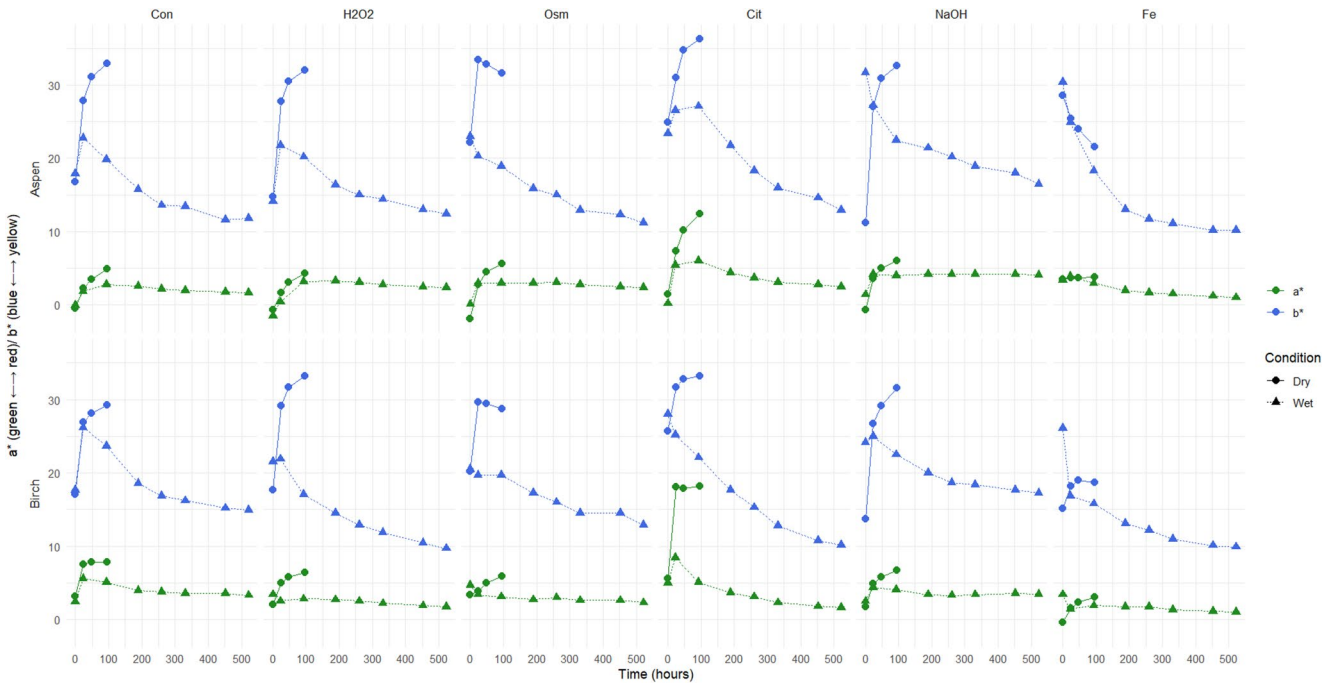

Fig. 3 Evolution of chromaticity values (a* and b*) by species, treatment and batch

of the test in all other treatments except the control samples and NaOH treatments, while in aspen it remained higher than at the beginning. In both wood species, yellowness decreased in the wet batch after the first day increase.

Greyness of the samples can be assessed with CIE-L*,a*,b* values. As a* and b* values monitor the chromaticity of materials, the closer they are to value 0, the greyer they are. In addition, L* value monitors lightness where 0 is completely black and 100 white, and the values between maximum and minimum express different shades of grey. Within these terms, Fe induced the most satisfactory greyness, as a* and b* were the closest to 0 (Fig. 3). As it was discussed, L* value Fe was the lowest of used treatment chemicals, between 50 and 60 (Fig. 2). Therefore, Fe

induced the most satisfactory greyness in terms of L*, a*, and b*, although the result was darker than naturally developed grey wood. Greyness mimicking natural weathering could be achieved by using lower concentrations of Fe.

3.3 Hyperspectral image data

Prior to artificial weathering, reflectivity among the samples was relatively uniform (Fig. 4). NaOH-treated specimens exhibited the lowest reflectivity, appearing darkest among all treatment types. In contrast, control (Con) samples were the most reflective. However, overexposure during imaging likely affected their apparent brightness. To avoid this in future studies, the use of light diffusers is recommended. In Fe-treated aspen samples, localized darkening was observed in areas where the iron solution had dried at higher concentrations, indicating uneven absorption. Spectral analysis revealed that reflectivity was lowest at 426 nm and increased steadily with wavelength, consistent with previous findings (Fig. 1). As shown in the hyperspectral (HS) images, distinct variation between earlywood and latewood is clearly visible—an important spatial detail that conventional spectrophotometers cannot detect due to their lack of spatial resolution. According to a review by Schimleck et al. (2023), VIS-NIR hyperspectral imaging systems have been applied in wood science for determining moisture content, classifying and detecting compression wood, measuring wood density, and identifying blue-stain fungi.

HSI shows similar spectral data as spectrophotometers, but in form of images containing greater spatial resolution. Therefore, spectrophotometer data (Fig. 1) and HS-images of the samples (Fig. 4) show similar spectral features. For instance, reflectance in the violet region is low and gradually increases towards infrared region. Con and Osm samples of Wet batch were similarly reflective (Fig. 4), and they were the most reflective samples of their batch. Cit and H2O2 of Wet batch were similarly reflective, and they were less reflective over Con and Osm. Con, Cit, H2O2, and NaOH

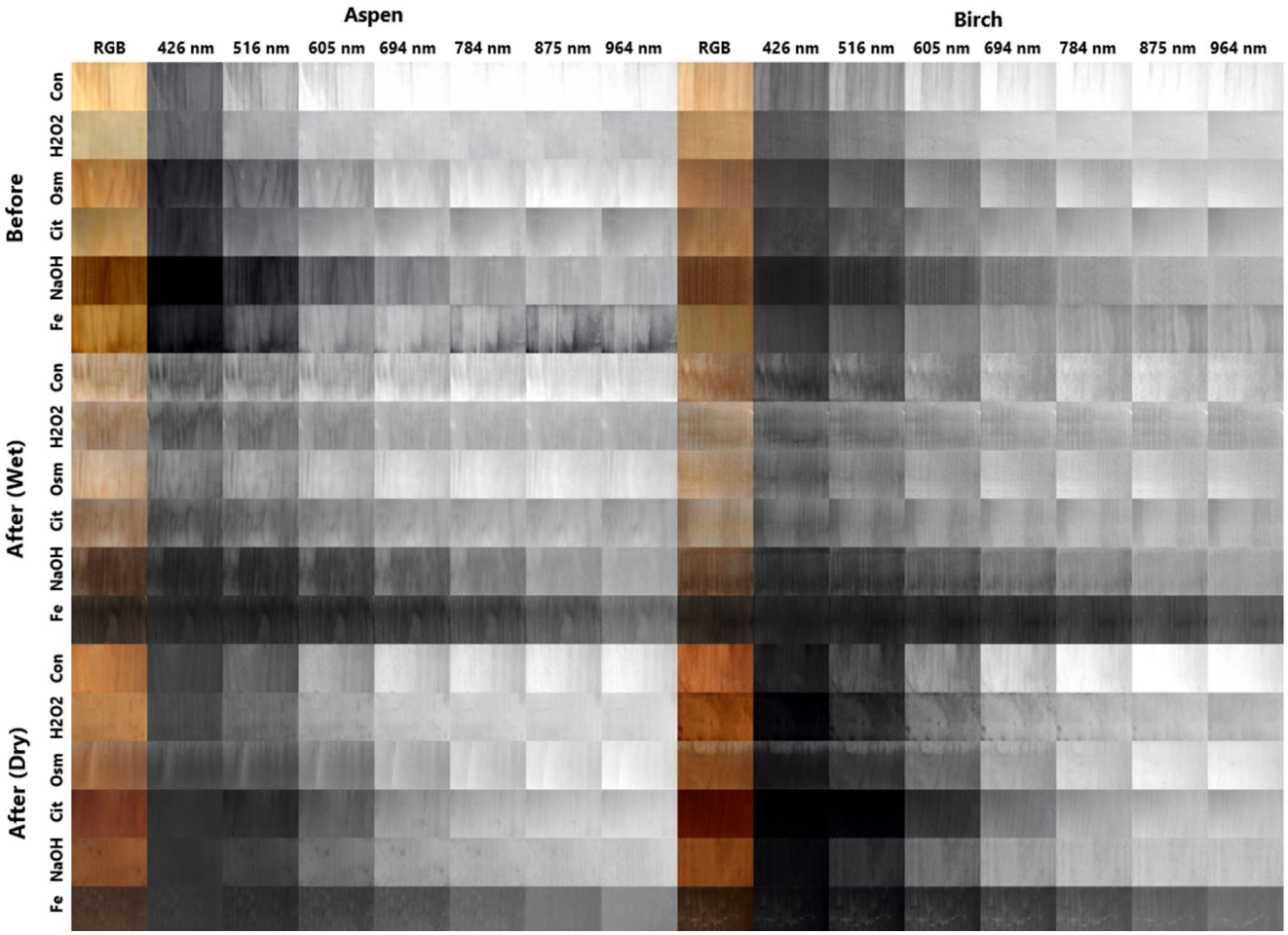

Fig. 4 Hyperspectral image panels of batch 2 (Wet) and batch 1 (Dry) in aspen (left) and birch (right) samples. The first image is an RGB image and the following images are hyperspectral images in which the corresponding wavelengths in nanometres are depicted. The corresponding colours of the wavelengths are as follows: 426 nm (violet), 516 nm (green), 605 nm (orange), 694 nm (red), 784 nm (IR), 875 nm (IR), and 964 nm (IR)

of Wet batch were more reflective at 426 nm when compared to samples before artificial weathering and Dry batch. This implies the absence of chromophoric compounds as discussed in earlier chapters. More distinct differences appeared in the NaOH and Fe samples. Fe samples were much darker than other samples. NaOH samples showed similar reflectivity from 426 to 784 nm wavelengths in both wood species (Fig. 4). From 784 to 964 nm wavelengths, the differences between reflectivity were less evident. Fe treatment was least reflective in the infrared region, suggesting a shift in maximum reflectance to longer wavelengths. The hyperspectral images in the violet region were darker in Dry batch than in Wet (Fig. 4), also implicating the presence of chromophoric compounds. Cit and Fe treated samples remained relatively dark, but Cit treated samples began to show greater reflectivity after 691 nm, following similar pattern to spectrophotometer data (Fig. 1). Lastly, HSI show considerable heterogeneous features in samples (Fig. 4), which is not detected by spectrophotometers (Fig. 1).

3.4 Spectrophotometer vs. hyperspectral image data in CIELAB colour space

HS-images were converted to CIELAB format, from which 6000 pixels per sample were chosen and converted to numeric values. Jordan et al. (2022) and Herrera-Díaz et al. (2018) conducted similar studies where they converted HSI data to CIE L*a*b* colour space. The L* (Fig. 5), a* (Fig. 6), and b* (Fig. 7) values were visualized as boxplots together with corresponding spectrophotometer data. The boxplots allow for comparison of the two methods used in this study. As expected, HSI recorded greater variability in all cases when compared spectrophotometer data. The median values recorded with the two methods are relatively close to each other in most cases (Figs. 5 and 6, and 7). Spectrophotometer recorded L* median values are greater in most cases (Fig. 5) as well as b* median values (Fig. 7). In the case of a* median values, spectrophotometer data expressed lower values when compared to HSI (Fig. 6). Boxplots in this case can be used to assess the evenness of induced colour change. H2O2 treatment before artificial weathering expressed the lowest variability in both wood species and all CIELAB values (Figs. 5 and 6, and 7). The largest variabilities were expressed by wet Fe and NaOH

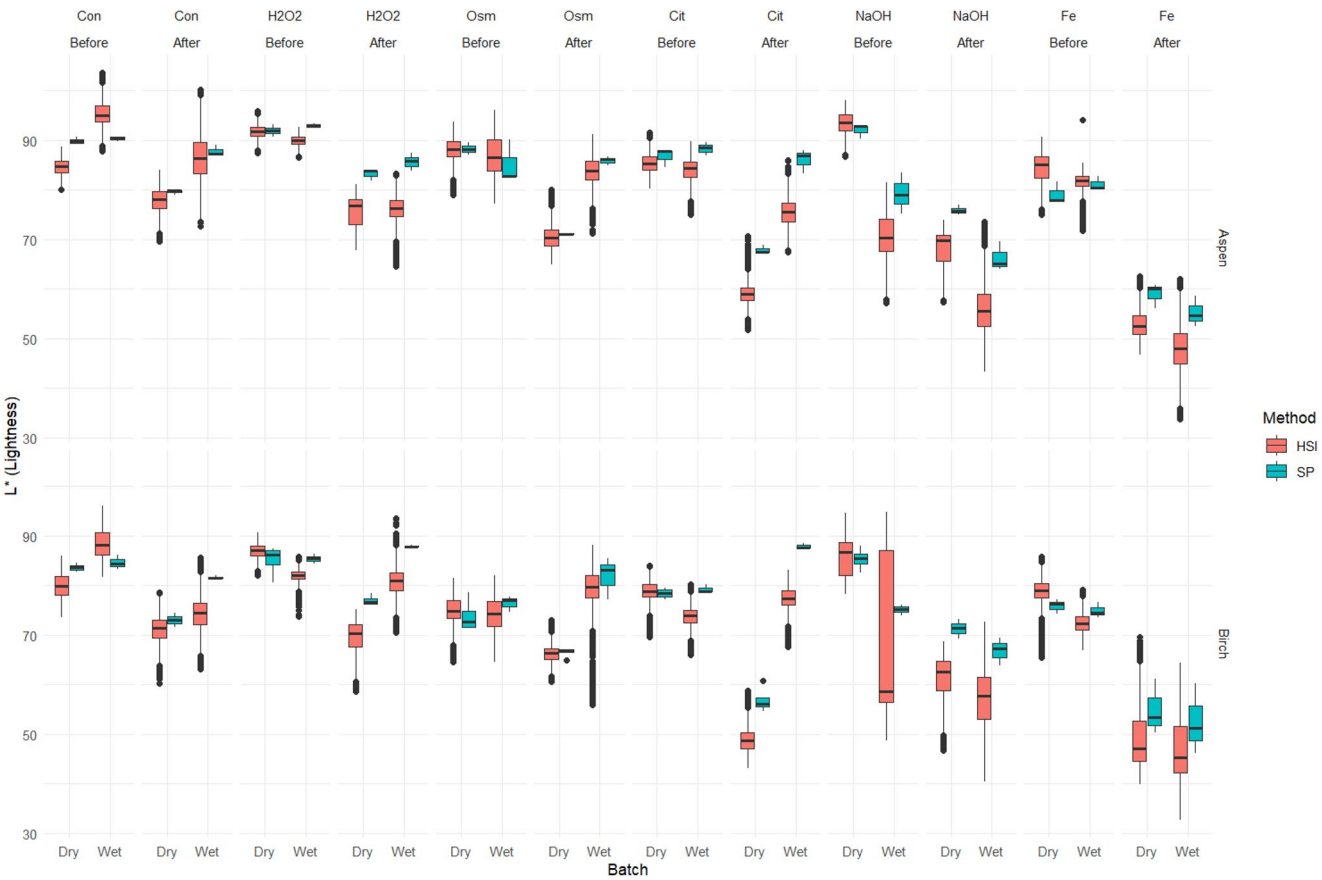

Fig. 5 Boxplots of lightness (L*) values differentiated by species, treatment, batch, and measurement method (HSI, SP = spectrophotometer)

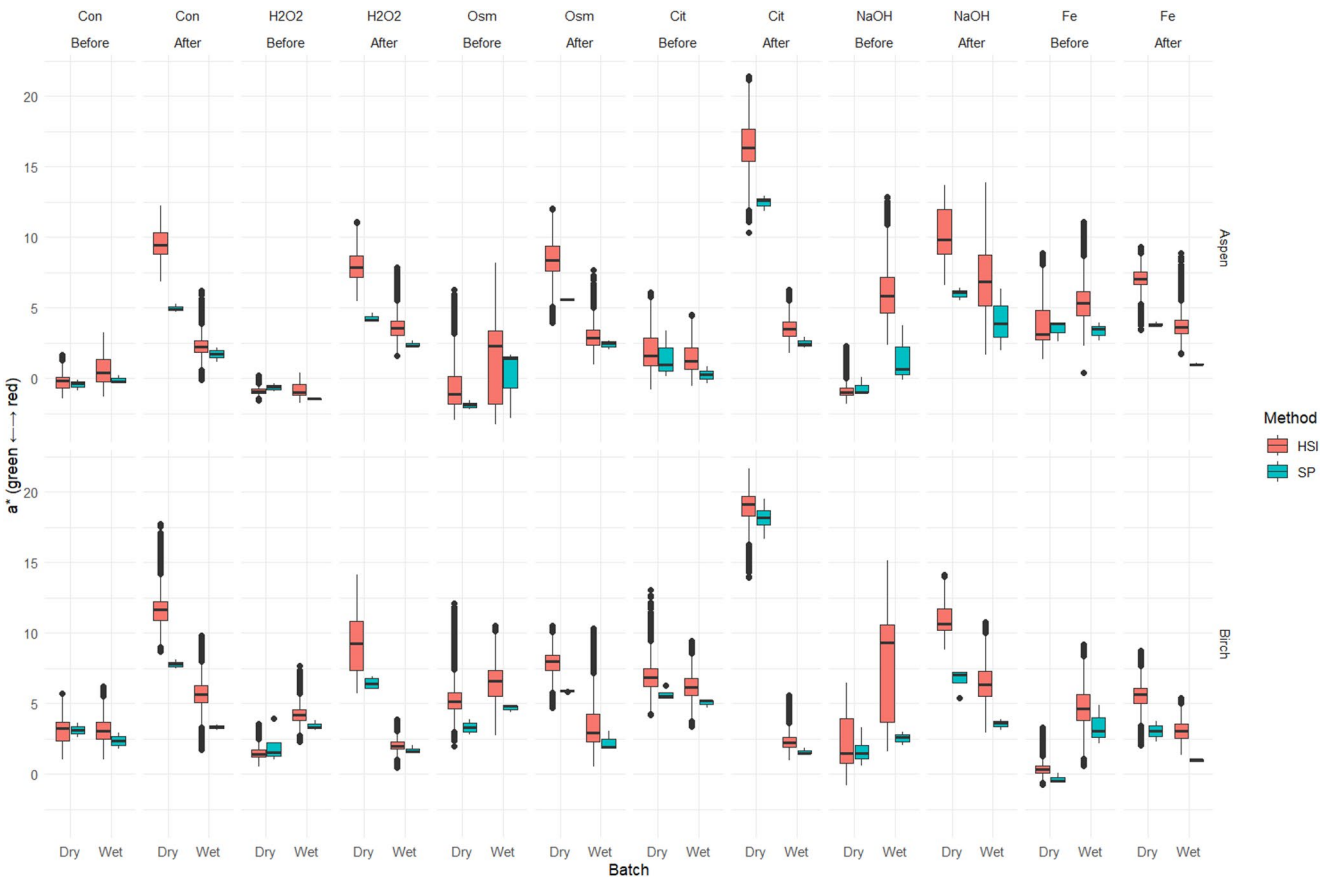

Fig. 6 Boxplots of a* values differentiated by species, treatment, batch, and measurement method (HSI, SP = spectrophotometer)

treatments. As it was shown in HS-images, NaOH caused uneven colouration with dirty appearance. Fe was mostly dark grey in colour, but lighter coloured spots were also apparent (Fig. 4). This has resulted in greater variability in L*, a*, and b* values.

It is assumed that spectrophotometers as standardized colour measuring instruments record colours more accurately. However, HSI data offers more colour measurement data points in the form of pixels compared to spectrophotometers, as HSI spatial data can capture larger areas of the test material and more heterogeneity. Spectrophotometers rely on point measurements and require multiple measurements to record heterogeneity accurately. In remote sensing, HSI has been used as a classification tool (Carbonneau and Piégay 2012). In tree research, classification of tree species based on hyperspectral stem bark images has been studied (Juola et al. 2023). For the studying of heterogeneous materials, such as wood, HSI offers more reflectance data about the variability within the test material. Herrera-Díaz et al. (2018) discussed the same advantages. Several factors can explain the differences of median values in this study. Wood, as heterogeneous material reflects light differently and measured reflectivity heavily depends on where the point measurement was taken. To overcome this uncertainty, increasing the amount of spectrophotometer datapoints would be required.

3.5 Effects of treatment chemicals

UV radiation induces photodegradation, including lignin degradation and photooxidation, resulting in the formation of carbonyl-containing chromophores (E.g., Timar et al. 2016). According to Tolvaj and Faix (1995), the yellow hue is primarily due to oligomeric chromophores, which are likely originated from leuco-chromophores of the lignin component of wood. Even short-term exposure triggers these changes, which develop over time according to patterns specific to the wood species. Although photodegradation induced a cumulative colour change in wood over relatively long periods of time, or in this case up to 522 h (Figs. 2 and 3), most sample types showed their greatest potential for colour change at the beginning of the weathering period, and the potential was smaller as weathering continued. The same phenomenon was also mentioned by Hon and Shiraishi 2001a, b; Jankowska et al. (2017); Sandak et al. (2017).

The 10% sodium hydroxide treatment (NaOH) of the wet batch prior to artificial weathering resulted in a pronounced

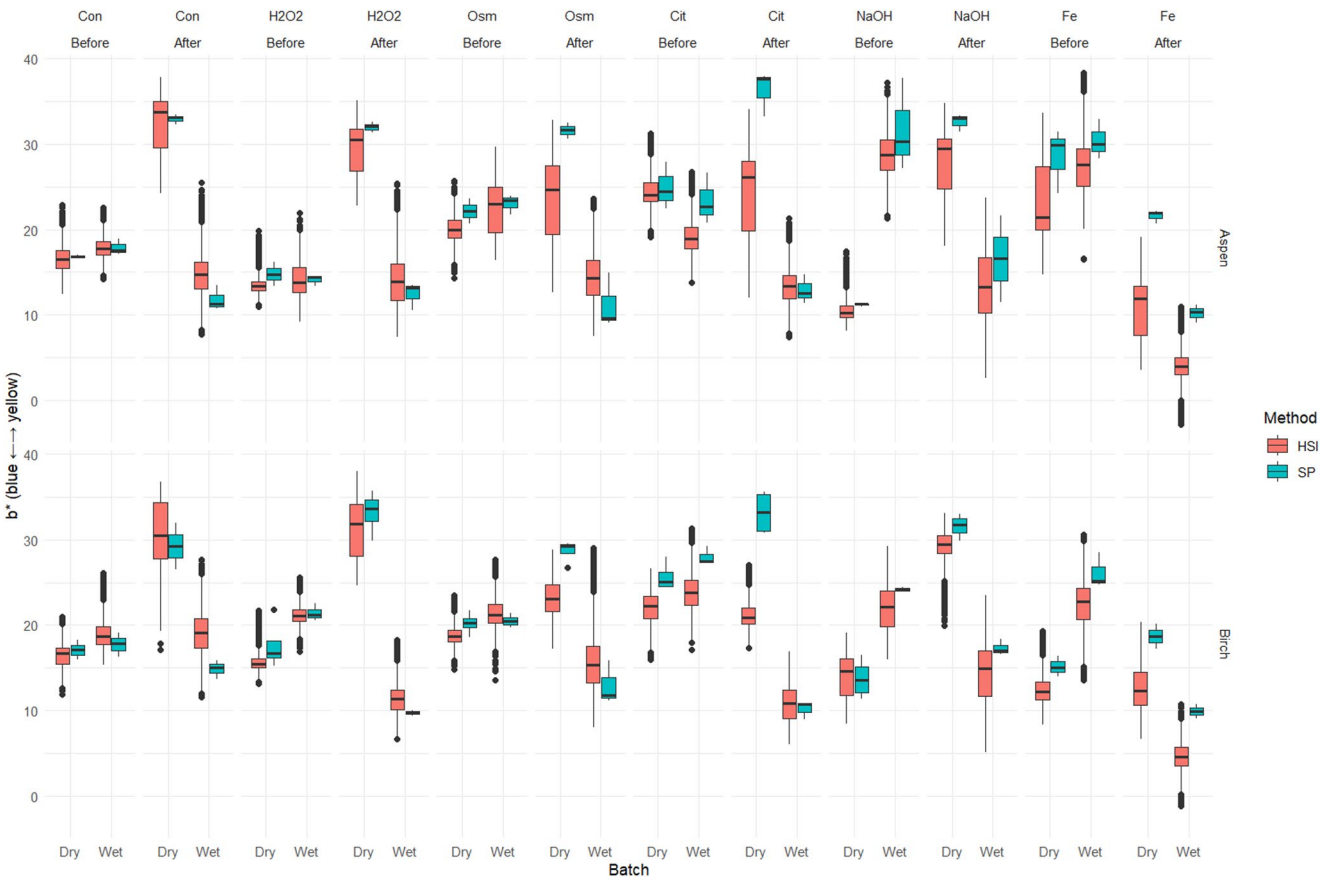

Fig. 7 Boxplots of b* values differentiated by species, treatment, batch, and measurement method (HSI, SP = spectrophotometer)

brown colouration compared to the control samples (Fig. 1). This result is in line with previous findings that high-pH alkaline treatments promote lignin oxidation and wood surface browning (Hon and Shiraishi 2001a, b; Qi et al. 2023). However, only a few studies have investigated the specific effects of NaOH treatment on the weathering behavior of wood. For example, Özçifçi and Özbay (2010) exposed Scots pine (*Pinus sylvestris*) and Oriental beech (*Fagus orientalis*) samples treated with 25% NaOH to outdoor weathering for 12 months, which resulted in noticeable darkening as was the case for both wood species in the wet batch of this study. In contrast, samples weathered without water spraying retained a yellowish-brown appearance with higher surface reflectance. It should be noted that this higher reflectivity in the dry batch is attributed to the 4% hydrogen peroxide treatment, which introduces a variable that precludes direct comparison of NaOH treatments between batches.

Citric acid (Cit) treatment increased redness of the samples, and the spectral reflectance increased in a similar way to Fe-treated wood up to 540 nm, beyond which the reflectance increased more steeply into the infrared region (Fig. 1). Acids are known to cause reddening of wood (Hon and Shiraishi 2001a, b), but the increased red colour due to decreased reflectivity at non-red wavelengths was unexpected. Few studies exist on citric acid in wood chemical modification and binding. Citric acid interacts with primary hydroxyl groups in lignin and polysaccharides, leading to esterification, enhancing bonding in wood adhesives (Umemura and Kawai 2015; Dunky 2020; Lee et al. 2020; Ando and Umemura 2020, 2021; Kurkowiak et al. 2022). Esterification reactions occur at aromatic and aliphatic hydroxyl groups of lignin and hemicellulose (Del Menezzi et al. 2018). Wang et al. (2021) studied decay resistance of poplar wood impregnated with citric acid-based water solution and reported reddening effect without UV light. Photochemical reactions between wood and citric acid causing red colour could be related to esterification of wood constituents and formation of chromophoric compounds. Furthermore, the red colour suggests the presence of conjugated double bonds and the resulting compounds from photochemical reactions are polar due to water leachability.

Hydrogen peroxide (H2O2) treatment effectively bleached the samples and increased their overall reflectivity, as expected due to its widespread use as a wood bleaching agent (Mononen et al. 2005a, b; Möttönen et al. 2003). After artificial weathering, the reflectance induced by H2O2 treatment increased in both the dry and wet batches, and

especially in the wet batch, more in birch than in aspen. For residual lignin, photochemical reactions together with hydrogen peroxide convert phenolic aromatic units into carboxylic acids and break down β-O-4 ether bonds, leading to lignin depolymerization (Perez et al. 2002). Hydrogen peroxide together with different catalysts can cause significant degradation of lignin and reduction in lignin content (Jung et al. 2015; D'Auria et al. 2018). In this study, hydrogen peroxide oxidized lignin, breaking its aromatic and chromophoric structure, thus causing bleaching. UV radiation further oxidized lignin and caused dry samples and wet birch samples to become more reflective over control samples. However, H2O2 caused the most even colour change prior to artificial weathering (Figs. 5 and 6, and 7), possibly due to superficial degradation of chromophoric lignin, causing homogeneous colour. Therefore, H2O2 could be used as surface treatment on uncoated wood to homogenise the wood surface and to prevent photolytic yellowing that occurs indoors. However, the use of H2O2 pre-weathering is not recommended, because the homogeneous colours were not resistant to photodegradation (Figs. 5 and 6, and 7). In addition, shortwave UV-light promotes the formation of hydroxyl radicals and hydrogen peroxide from water and oxygen (Azrague et al. 2005), making the supplementary hydrogen peroxide redundant.

The reflectance behaviour of Organowood (Osm) treated samples in the wet batch was similar to that of the control samples. In the dry batch, the changes were even smaller than those of the control samples. Thus, the Osm treatment did not accelerate greying or other colour changes during weathering. Organowood contains silicon compounds in a highly alkaline aqueous solution. Sodium silicate is manufactured with quartz and sodium hydroxide solution. As a result, the solution reacts and forms sodium orthosilicate and -metasilicate. Sodium silicate has been used as wood fire retardant (Giudice and Pereyra 2007; Pries and Mai 2013). It appears that the active silicon compounds of Organowood treatment that noticeably altered the reflectance of wood post-treatment were mostly lost during the weathering when samples were subjected to altering wet conditions. Hence, Osm treatment failed to induce a permanent colour change in either wood species. It is possible that the ultra-pure water used for spraying dissolved and leached the active compounds of Osm.

Iron (II) sulphate or $FeSO_4$null is known to darken wood, producing a grey tone resembling weathered surfaces (Hon and Shiraishi 2001a, b). In woodworking, a common method to stain wood to accomplish black finish is referred to as ebonizing, which in many cases includes the use of iron and tannins from different sources (Kukreti et al. 2024). Several studies have explored the use of $FeSO_4$ on wood together with weathering (Hundhausen et al. 2020; Lesar and Humar 2022; Jankowska and Kwiatkowski 2022; Dagher et al. 2022, 2023; Lesar et al. 2024). The catalytic properties of iron in $FeSO_4$ further facilitate the breakdown of lignocellulosic materials (Kim et al. 2024). $FeSO_4$ pretreatment significantly enhances the degradation of hemicellulose, and the pretreatment process disrupts ester linkages between cellulose and hemicellulose, breaking the structure of lignocellulosic biomass (Zhao et al. 2011). The low reflectance across the visible range of Fe-treated samples shows as a dark grey colour, shown in the RGB images (Fig. 1) and HS-images (Fig. 4). UV-light accelerated the staining effect since it was not observed before artificial weathering, as also reported by Hundhausen et al. (2020). Their study further discussed the possible reasons behind the staining effects of $FeSO_4$ and concluded that iron ions are oxidated by photodegraded lignin constituents such as phenoxy and ketyl radicals. However, they did not consider any chemical bonding between wood components as staining caused by $FeSO_4$ was not prone to leaching caused by water. Also, the results in this study (Figs. 2 and 3) imply that staining caused by $FeSO_4$ is not prone to water leaching. Furthermore, in Hundhausen et al. (2020) study acetylated radiata pine and thermally treated pine and ash showed less staining, presumably due to hindered penetration caused by changes in the cell wall. An alternative mechanism for the staining effect is proposed here. It is likely that the staining effect is similar to that of historical iron gall ink, which is composed of $FeSO_4$ and gallotannins obtained from galls of oak trees. Iron gall ink is resistant to water but it also degrades cellulose based papers (Çakar and Akyol 2022; Melo et al. 2022). UV-light promotes the formation of reactive oxygen species, facilitating oxidising of Fe^{+2} to Fe^{+3}, and mimicking Fenton reactions (Jung et al. 2015). Both Fe^{+2} and its oxidised form Fe^{+3} play a role in catalysing the degradation of glycosidic bonds of cellulose and promoting the formation of poly-galloyl glucoses. These are formed by esterification of glucose monomers and gallic acids (Melo et al. 2022; Ferretti et al. 2024). In the context of wood weathering, iron ions of $FeSO_4$ may play a similar catalytic role, whereas the photodegraded lignin constituents may play the role of phenolic acids. Fe ions oxidise and cleave glycosidic bonds of cellulose but also catalyse the formation of ester bonds between hydroxyl groups of cellulose and phenolic acids of photodegraded lignin. This is supported by the results of Hundhausen et al. (2020) regarding acetylated wood, thermally treated wood and wood samples free of tannins. As hydroxyl groups of cellulose in acetylated wood have been substituted by acetyl groups, and those of thermally treated wood have been thermally degraded, they cannot form such ester bonds and thus cannot be stained by iron in this way. Furthermore, despite the absence of tannins, $FeSO_4$ nevertheless caused staining in their study, suggesting staining by

photodegraded lignin. Further chemical analyses should be conducted to affirm this. If cellulose chains remain intact to high enough degree, the reaction could be utilised to promote tannin fixation and decay resistance of wood. Furthermore, in the context of biorefining, UV-induced photolysis together with iron catalysts could be used in the synthesis of economically valuable biochemicals.

The results show that the use of water spraying as an aid to UV irradiation would be important when weathering-induced colour changes of wood are artificially produced on an industrial scale. Artificial UV aging without water did not produce a colour change that mimic natural greying but rather yellowing that takes place indoors. On the other hand, $FeSO_4$ and citric acid in dry conditions and hydrogen peroxide prior to artificial weathering produced interesting finishes that could have economic value.

4 Conclusion

This study provides insights into the effects of UV light and treatment chemicals on the colour changes in wood using a novel hyperspectral imaging (HSI), suggesting potential applications and future research directions for understanding and utilizing these phenomena. Most of the tested chemicals successfully yielded distinct discolouration profiles: $FeSO_4$ induced uniform dark grey staining, sodium hydroxide produced a brown hue, hydrogen peroxide treated samples showed the most consistent colour change, and citric acid generated a warm reddish tone, particularly under dry UV exposure. Introducing water during the artificial weathering process showed an increase in reflectivity in the UV region, indicating the leaching effect of water on chromophoric compounds. The presence of water increased the light tones and greyness of wood, whereas the exclusion of water made the wood darker and, in most cases, increased yellow colouration. Hydrogen peroxide treatment effectively bleached the wood samples, but this effect did not last after the weathering trials. Organowood ® did not induce a significant colour change, possibly due to the dissolution of its active compounds during the weathering process. $FeSO_4$ treatment consistently resulted in dark grey colouration.

HSI-system showed its capability and advantages over spectrophotometric methods in this study. From a methodological perspective, HSI offered greater spatial detail and sensitivity to heterogeneity than traditional point-based spectrophotometry. The combination of reflectance and spatial data in HSI-systems can be a competitive alternative in colour measurement.

Future research directions are suggested, including studying photochemical reactions induced by visible light, exploring the use of gaseous compounds and photochemical reactions to form unique colours or modified wood. As xenon lamps used in this study are costly, economic alternatives to expensive UV light sources, such as powerful LED lights, should be assessed. Iron catalysed tannin fixation to cellulose should be further studied, in relation to wood decay resistance. Further research should explore the potential of photochemical reactions as biorefining method for lignocellulosic materials. The use catalysts such as organic acids or metal salts is suggested.

Acknowledgements Puumiesten ammattikasvatussäätiö (The Foundation for Finnish Wood Professionals' Education) has funded this project. Part of the writing of this article was done in the framework of the Puu-TKI project (Grant nr A80321) funded by the Regional Council of North Karelia under the theme Innovative Finland.JL was funded by The Finnish Society of Forest Science, grant nr: 20240040.MK was supported by Research Council of Finland Flagship Programme, Photonic Research and Innovation (PREIN), decision 346518.

Author contributions J.L. wrote the main manuscript. J.L. and V.M. planned and carried out the UV weathering treatments and spectrphotometer measurements. J.L., M.K. and O.A. carried out the hyperspecral measurements and analysis. J.L., and M.K. prepared the figures and tables. All authors took part in the studies construction and interpretation of data.

Funding Open access funding provided by Natural Resources Institute Finland. Puumiesten ammattikasvatussäätiö (The Foundation for Finnish Wood Professionals' Education) has funded this project. Part of the writing of this article was done in the framework of the Puu-TKI project (Grant nr A80321) funded by the Regional Council of North Karelia under the theme Innovative Finland. JL was funded by The Finnish Society of Forest Science, grant nr: 20240040. MK was supported by Research Council of Finland Flagship Programme, Photonic Research and Innovation (PREIN), decision 346518.

Data availability No datasets were generated or analysed during the current study.

Declarations

Conflict of interest The authors declare no competing interests.

Open Access This article is licensed under a Creative Commons Attribution 4.0 International License, which permits use, sharing, adaptation, distribution and reproduction in any medium or format, as long as you give appropriate credit to the original author(s) and the source, provide a link to the Creative Commons licence, and indicate if changes were made. The images or other third party material in this article are included in the article's Creative Commons licence, unless indicated otherwise in a credit line to the material. If material is not included in the article's Creative Commons licence and your intended use is not permitted by statutory regulation or exceeds the permitted use, you will need to obtain permission directly from the copyright holder. To view a copy of this licence, visit http://creativecommons.org/licenses/by/4.0/.

References

Ando D, Umemura K (2020) Bond structures between wood components and citric acid in wood-based molding. Polymers 13(1):1–9. https://doi.org/10.3390/polym13010058

Ando D, Umemura K (2021) Chemical structures of adhesive and interphase parts in sucrose/citric acid type adhesive wood-based molding derived from Japanese Cedar (*Cryptomeria japonica*). Polymers 13(23):4224. https://doi.org/10.3390/polym13234224

Azrague K, Bonnefille E, Pradines V, Pimienta V, Oliveros E, Maurette M-T, Benoit-Marquié F (2005) Hydrogen peroxide evolution during V-UV photolysis of water. Photochem Photobiol Sci 4(5):406–408. https://doi.org/10.1039/b500162e

Çakar P, Akyol E (2022) The effects of natural dye and iron gall ink on degradation kinetics of cellulose by accelerated ageing. Stud Conserv 67(6):381–388. https://doi.org/10.1080/00393630.2021.1996090

Carbonneau P, Piégay H (2012) Fluvial remote sensing for science and management, 1st edn. Wiley

Dagher R, Stevanovic T, Landry V (2022) Photostability of white oak wood stained with metal salts during indoor sunlight exposure. Eur J Wood Prod 80(2):313–330. https://doi.org/10.1007/s00107-021-01775-2

Dagher R, Stevanovic T, Landry V (2023) Wood color modification with iron salts aqueous solutions: effect on wood grain contrast and surface roughness. Holzforschung 77(5):356–367. https://doi.org/10.1515/hf-2022-0189

D'Auria M, Mecca M, Todaro L (2018) Lignin and extractives degradation in Poplar wood in the presence of hydrogen peroxide and molybdenum polyoxometalated compound. Eur J Wood Prod 76(5):1527–1533. https://doi.org/10.1007/s00107-018-1334-8

Del Menezzi C, Amirou S, Pizzi A, Xi X, Delmotte L (2018) Reactions with wood carbohydrates and lignin of citric acid as a bond promoter of wood veneer panels. Polymers 10(8):833. https://doi.org/10.3390/polym10080833

Dunky M (2020) Wood adhesives based on natural resources: A critical review: part II. carbohydrate-based adhesives. Reviews Adhes Adhes 8(3):333–378. https://doi.org/10.7569/RAA.2020.097310

Fengel D, Wegener G (1984) Wood: chemistry, ultrastructure, reactions. de Gruyter, Berlin, pp 348–349

Ferretti A, Sabatini F, Degano I (2024) Linking historical recipes and ageing mechanisms: the issue of 19th century iron gall inks. J Cult Herit 67:111–120. https://doi.org/10.1016/j.culher.2024.02.012

Giudice CA, Pereyra AM (2007) Fire resistance of wood impregnated with soluble alkaline silicates. Res Lett Mater Sci Article ID 31956:4. https://doi.org/10.1155/2007/31956

Herrera R, Sandak J, Robles E, Krystofiak T, Labidi J (2018) Weathering resistance of thermally modified wood finished with coatings of diverse formulations. Prog Org Coat 119:145–154. https://doi.org/10.1016/j.porgcoat.2018.02.015

Hon DN, Shiraishi N (2001a) Wood and cellulosic chemistry (2nd ed., rev. and expanded.). New York: Marcel Dekker. pp 385–409

Hon DN-S, Shiraishi N (2001b) Wood and cellulosic chemistry, 2nd edn. Marcel Dekker. rev. expanded.

Hundhausen U, Mai C, Slabohm M, Gschweidl F, Schwarzenbrunner R (2020) The staining effect of iron (II) sulfate on nine different wooden substrates. Forests 11(6):658. https://doi.org/10.3390/f11060658

ISO 16474-2 (2013) Paints and varnishes. Methods of exposure to laboratory light sources. Part 2: xenon-arc lamps. International Standards Organisation, Geneva

Jankowska A, Kwiatkowski A (2022) Effectiveness of European oak wood staining with iron (II) sulphate during natural weathering. Maderas 24:1–10. https://doi.org/10.4067/S0718-221X2022000100415

Jankowska A, Reder M, Gołofit T (2017) Comparative study of wood color stability using accelerated weathering process and infrared spectroscopy. Wood Res 62(4):549–556

Jordan J, Helander R, Laaksonen P (2022) Colour stability of wood coatings pigmented with natural Indigo from *Isatis tinctoria* after accelerated weathering. Color Technol 138(2):210–218. https://doi.org/10.1111/cote.12585

Jung YH, Kim HK, Park HM, Park Y-C, Park K, Seo J-H, Kim KH (2015) Mimicking the Fenton reaction-induced wood decay by fungi for pretreatment of lignocellulose. Bioresour Technol 179:467–472. https://doi.org/10.1016/j.biortech.2014.12.069

Juola J, Hovi A, Rautiainen M (2023) Classification of tree species based on hyperspectral reflectance images of stem bark. Eur J Remote Sens ahead–of–print(ahead–of–print):1–15. https://doi.org/10.1080/22797254.2022.2161420

Kataoka Y, Kiguchi M, Williams RS, Evans PD (2007) Violet light causes photodegradation of wood beyond the zone affected by ultraviolet radiation. Holzforschung 61(1):23–27. https://doi.org/10.1515/HF.2007.005

Kim E, Yoon K, Kwon G, Kim N, Park G, Jeon YJ, Kwon EE, Song H (2024) Thermo-chemical upcycling of cellulosic paper packaging waste into furfural and bio-fuel catalyst. J Anal Appl Pyrol 183:106844. https://doi.org/10.1016/j.jaap.2024.106844

Konica Minolta (2007) Precise color communication. Color control from feeling to instrumentation. Konica Minolta Sensing Inc., Japan. https://www.konicaminolta.com/instruments/knowledge/color/pdf/color_communication.pdf

Kukreti SB, Ayate D, Kukreti SB (2024) An insight into Ebony and ebonization of wood. Appl Biol Res 26(2):143–151. https://doi.org/10.48165/abr.2024.26.01.18

Kurkowiak K, Emmerich L, Militz H (2022) Wood chemical modification based on bio-based Polycarboxylic acid and polyols - status quo and future perspectives. Wood Mater Sci Eng 17(6):1040–1054. https://doi.org/10.1080/17480272.2021.1925961

Lee SH, Tahir PM, Lum WC, Tan LP, Bawon P, Park B-D, Osman Al Edrus SS, Abdullah UH (2020) A review on citric acid as green modifying agent and binder for wood. Polymers 12(8):1692. https://doi.org/10.3390/POLYM12081692

Lesar B, Humar M (2022) Performance of iron(II)-sulphate-treated Norway Spruce and Siberian larch in laboratory and outdoor tests. Forests 13(9):1497. https://doi.org/10.3390/f13091497

Lesar B, Humar M, Osvald F (2024) Colour changes of weathered wood surfaces before and after treatment with iron (II) sulphate. Drvna Industrija 75(1):5–17. https://hrcak.srce.hr/314750

Lv S, Liang S, Zuo J, Zhang S, Wang J, Wei D (2023) Lignin-based anti-UV functional materials: recent advances in Preparation and application. Iran Polym J 32(11):1477–1497. https://doi.org/10.1007/s13726-023-01218-0

Melo MJ, Otero V, Nabais P, Teixeira N, Pina F, Casanova C, Fragoso S, Sequeira SO (2022) Iron-gall inks: a review of their degradation mechanisms and conservation treatments. Herit Sci 10(1). https://doi.org/10.1186/s40494-022-00779-2. Article 145

Miklecic J, Jirous-Rajkovic V (2011) Accelerated weathering of coated and uncoated Beech wood modified with citric acid. Drvna Industrija 62(4):277–282. https://doi.org/10.5552/drind.2011.1116

Mitsui K (2004) Changes in the properties of light-irradiated wood with heat treatment: part 2. Effect of light-irradiation time and wavelength. Eur J Wood Prod 62(1):23–30. https://doi.org/10.1007/s00107-003-0436-z

Mononen K, Alvila L, Pakkanen TT (2005a) Changes in color and structure of Birch wood (*Betula pendula*) caused by bleaching with hydrogen peroxide solution. Holzforschung 59(1):59–64. https://doi.org/10.1515/HF.2005.010

Mononen K, Jääskeläinen A-S, Alvila L, Pakkanen TT, Vuorinen T (2005b) Chemical changes in silver Birch (*Betula pendula* Roth) wood caused by hydrogen peroxide bleaching and monitored by color measurement (CIELab) and UV-Vis, FTIR and UVRR spectroscopy. Holzforschung 59(4):381–388. https://doi.org/10.1515/HF.2005.063

Möttönen V, Asikainen A, Malvaranta P, Öykkönen M (2003) Peroxide bleaching of parquet blocks and glue lams. Holzforschung 57(1):75–80. https://doi.org/10.1515/HF.2003.012

Möttönen V, Boren H, Heräjärvi H (2018) Puun ominaisuuksien modifiointi: Menetelmät ja tutkimuksen tila (Modification of wood properties: Methods and state of research). Luonnonvara- ja biotalouden tutkimus 11/2018. Luonnonvarakeskus, Helsinki. 57 p. https://jukuri.luke.fi/bitstream/handle/10024/541544/luke-luobio_11_2018.pdf?sequence=1&isAllowed=y

Özçifçi A, Özbay G (2010) Impacts of bleaching chemicals and outdoor exposure on changes in the color of some varnished woods. BioResources 5(2):586–597

Park S-Y, Hong C-Y, Kim S-H, Choi J-H, Kwon O, Lee H-J, Choi I-G (2018) Photodegradation of natural wood veneer and studies on its color stabilization for automotive interior materials. J Wood Chem Technol 38(4):301–312. https://doi.org/10.1080/02773813.2018.1488872

Perez DD, Silva, Castellan A, Nourmamode A, Grelier S, Ruggiero R, Machado EH (2002) Photosensitized delignification of residual lignin and chemical pulp from Eucalyptus grandis wood. Holzforschung 56(6):595–600. https://doi.org/10.1515/HF.2002.091

Pries M, Mai C (2013) Fire resistance of wood treated with a cationic silica Sol. Eur J Wood Prod 71:237–244

Qi Y, Zhou Z, Xu R, Dong Y, Zhang Z, Liu M (2023) Effect of NaOH pretreatment on permeability and surface properties of three wood species. ACS Omega 8(43):40362–40374. https://doi.org/10.1021/acsomega.3c04745

Rowell RM (2005) Handbook of wood chemistry and wood composites. CRC. https://doi.org/10.1201/9780203492437

Rowell RM (2013) Handbook of wood chemistry and wood composites, 2nd edn. Taylor & Francis, Boca Raton, pp 151–172

Sandak A, Burud I, Sandak J (2017) Hyperspectral imaging of weathered wood samples in transmission mode. Int Wood Prod J 8(1suppl):9–13. https://doi.org/10.1080/20426445.2016.1237079

Schimleck L, Ma T, Inagaki T, Tsuchikawa S (2023) Review of near infrared hyperspectral imaging applications related to wood and wood products. Appl Spectrosc Rev 58(9):585–609. https://doi.org/10.1080/05704928.2022.2098759

Schindelin J, Arganda-Carreras I, Frise E, Kaynig V, Longair M, Pietzsch T, Preibisch S, Rueden C, Saalfeld S, Schmid B, Tinevez J-Y, White DJ, Hartenstein V, Eliceiri K, Tomancak P, Cardona A (2012) Fiji: an open-source platform for biological-image analysis. Nature Methods 9:676–682. https://doi.org/10.1038/nmeth.2019

Timar MC, Varodi AM, Gurău L (2016) Comparative study of photodegradation of six wood species after short-time UV exposure. Wood Sci Technol 50:135–163. https://doi.org/10.1007/s00226-015-0771-3

Tolvaj L, Faix O (1995) Artificial ageing of wood monitored by DRIFT spectroscopy and CIEL*a*b* color measurements. Holzforschung 49:397–404

Umemura K, Kawai S (2015) Development of Wood-Based materials bonded with citric acid**. For Prod J 65(1–2):38–42. https://doi.org/10.13073/FPJ-D-14-00036

Wang J, Zhenju BI, Chen Z, Li YAN, Yafang LEI (2021) Decay resistance, dimensional stability and mechanical strength of Poplar wood modified with plant-derived compounds. Wood Res 66(4):556–568. https://doi.org/10.37763/WR.1336-4561/66.4.556568

Zhao J, Zhang H, Zheng R, Lin Z, Huang H (2011) The enhancement of pretreatment and enzymatic hydrolysis of corn Stover by $FeSO_4$ pretreatment. Biochem Eng J 56(3):158–164. https://doi.org/10.1016/j.bej.2011.06.002

Publisher's note Springer Nature remains neutral with regard to jurisdictional claims in published maps and institutional affiliations.